Electronic Supplementary Information

Tailored coordination nanoparticles: assessing the magnetic single-domain critical size

Yoann Prado,[a] Laurent Lisnard,[a] Daniela Heurtaux,[a] Guillaume Rogez,[b] Alexandre Gloter,[c] Odile Stéphan,[c] Nada Dia,[a] Eric Rivière,[a] Laure Catala[a,*] and Talal Mallah[a,*]

Experimental

The Scanning Transmission Electron Microscopy in the High Angular Dark field (STEM-HAADF) mode and Scanning Transmission Electron Microscopy in Electron Energy Loss Spectroscopy (STEM-EELS) modes have been performed with a dedicated scanning transmission electron microscope (Vacuum Generators HB501) equipped with a home modified Gatan spectrometer. All spectra are recorded in STEM mode with 100 keV incident electrons focused on the specimen. The probe size is at around 0.8 nm and the current intensity varies from 100 to 300 pA depending on the surface condition of the emitting tip. With such an equipment, spectra with energy range for 200 eV to 900 eV can be collected in several tens of milliseconds when chemical map is done (for instance when 32x32 spectra are collected) or in few seconds when higher signal to noise ratio are required.
The N and Cr maps have been obtained after a conventional Egerton edge removal technique. The Cs and Ni maps, whose spectra are superimposed, have been obtained by a non linear square fitting procedure using reference spectra.
The HRTEM measurements have been done on a TEM JEOL 2010 equipped with an ultra high resolution pole piece (Cs at around 0.5 mm). When necessary, in order to limit the irradiation damage, HRTEM images have been done while keeping the sample at LN2 temperature.
The TEM measurements have been done on a TEM Philips EM208 with 100 keV incident electrons focused on the specimen.
The Dynamic light scattering measurement has been performed on a Malvern Nanozetasizer Apparatus (equipped with a backscattering mode) on the aqueous solutions containing the particles. The volume profile was used to estimate the size corresponding to the main peaks. This measurement was used as a qualitative measurement of the size of the particles or aggregates in solution, which systematically includes a solvation shell. It provides a comparative measurement to follow growth of the multishell particles in solution.
X-ray Powder diffraction (XRPD) was performed on powders deposited on an aluminium plate and collected on a Philipps Panalytical X'Pert Pro MPD powder diffractometer at CuKα radiation equipped with a fast detector.
Magnetic measurements were carried out with a Quantum Design MPMS-5S magnetometer working in the dc mode and on a Quantum Design MPMS-XL magnetometer with an oscillating field of 3 Oe in the ac mode.

Calculation of the size of the core-shell targeted particles

Since the core and the shell have the same structure, we can safely assume that the atomic density of the core and the core-shell particles are the same. Thus we can write:

$N_C/V_C = N_{C\text{-}S}/V_{C\text{-}S}$ (1)

where N_C and V_C are respectively the number of atoms and the volume of the core particles ; and $N_{C\text{-}S}$ and $V_{C\text{-}S}$ are respectively the number of atoms and the volume of the core-shell particles. The number of atoms for the core-shell particles is the sum of that of the core and the shell, thus:

$N_{C\text{-}S} = N_C + N_S$ (2)

Equation (1) can be written in the following form:

$V_{C\text{-}S}/V_C = (N_C + N_S)/N_C = 1 + N_S/N_C$ (5)

For cubic particles of a side a, equation (5) becomes $a^3_{C\text{-}S}/a^3_C = 1 + N_S/N_C$

and hence : $a_{C\text{-}S} = a_C\,(1+ N_S/N_C)^{1/3}$ (6)

The same relation stands for the number of moles of atoms (n), thus:

$a_{C\text{-}S} = a_C\,(1+ n_S/n_C)^{1/3}$ (7)

Equation (7) gives the relation to calculate the number of moles of atoms n_S that must be added to the solution of core particles with a size a_C which contain a number of moles of atoms n_C in order to grow core-shell particles with a size $a_{C\text{-}S}$.

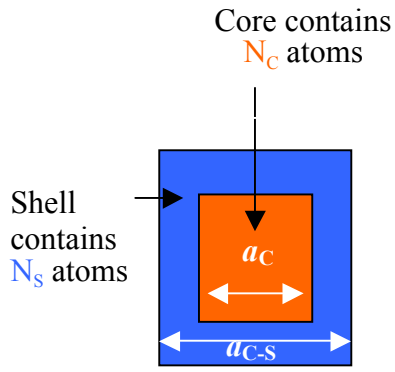

Synthetic procedure

Synthesis of 6 nm CsNiCr nanoparticles sample [6]

These "seed" nanoparticles were synthesized as reported in [27]. An aqueous solution (100 ml) containing of $NiCl_2.6H_2O$ (0.2 mmol, 2 mM) and CsCl (0.4 mmol, 4 mM) was added rapidly in an equal volume of aqueous solution of $K_3Cr(CN)_6$ (0.2 mmol, 2mM) under vigorous stirring. The solution was stirred for one hour and checked by Dynamic Light Scattering (see Fig. S1).

n_S/n_C indicates the ratio between the number of moles contained in the core (n_C) and shell (n_S), as used in the calculation reported above.

Synthesis of 8 nm CsNiCr nanoparticles [8]

Calculated ratio $\mathbf{n_S/n_C=1.2}$

From the as prepared 6 nm CsNiCr nanoparticles, an aqueous solution (*150 mL*) of $NiCl_2.6H_2O$ (*0.6 mmol*, *2 mM*) and CsCl (*1.2 mmol, 4 mM*) and an aqueous solution (*150 mL*) of $K_3Cr(CN)_6$ (*0.6 mmol, 2 mM*) were added in a drop wise manner under stirring at room temperature.

Growth of 10, 12, 16, 18, 22 and 30 nm sized CsNiCr nanoparticles

In a same way, an aqueous solution of $NiCl_2.6H_2O$ and CsCl (2 mM and 4 mM respectively) and a 2 mM aqueous solution of $K_3Cr(CN)_6$ were added drop wise to a solution of **[6]** with different ratio n_S/n_C (=3.6, 7, 18, 21.7, 48.3,136.9) to obtain samples **[10], [12], [16], [18], [22], [30]** respectively.

Isolation of the particles

In order to characterize the different samples and to study their magnetic behavior, we prepared two types of samples by dividing each preparation into two parts. The first solution was treated with Dioctadecyl dimethyl ammonium bromide (DODABr) to recover the particles surrounded by $DODA^+$ as a powder (eventually redispersable) for infra-red, Transmission Electron Microscopy (TEM) imaging, X-ray powder diffraction (XRPD) studies and for the elemental analysis. The second solution was recovered by using the organic polymer Polyvinylpyrrolidone (PVP) diluting as much as possible the nanoparticles (see below for details) in order to minimize interparticle interactions, which is crucial for the magnetic studies.

In order to characterize the different samples and to study their magnetic behaviour, we prepared two types of samples by dividing each preparation into two parts. One part was treated with Dioctadecyl dimethyl ammonium bromide (DODABr) to recover the particles surrounded by $DODA^+$ as a powder (eventually redispersable) for infra-red, Transmission Electron Microscopy (TEM) imaging, X-ray powder diffraction (XRPD) studies and for the elemental analysis. The second part was treated by the organic polymer Polyvinylpyrrolidone (PVP) diluting as much as possible the nanoparticles (see synthetic procedure) in order to minimize interparticle interactions. It is important to stress that since the dilution of the particles within the PVP matrix is constant for the different samples, the dipolar interaction increases when the size of the particles increases. This effect means that the we are able to determine only a lower limit of the single domain size.

Particles coated with a DODA$^+$ layer

The freshly prepared aqueous solution of nanoparticles was added drop wise to a methanolic solution (0.5 mM) containing dimethyldioctadecylammonium bromide (DODABr), with a constant volume ratio (2.5) between methanol and water. The flocculated particles were centrifuged at 8000 rpm during 15 min and the resulting blue-green powder was dried under vacuum.

Particles embedded in polyvinylpyrrolidone (PVP)

To the freshly prepared aqueous solution of nanoparticles, 300 equivalents of PVP (repeating unit MW =111 g.mol^{-1}) per divalent metallic ion were added to the solution of nanoparticles. 3 volumes of acetone with respect to the volume of the particles solution were added. The flocculated particles were centrifuged at 8000 rpm during 15 min and the resulting solid was dried under vacuum.

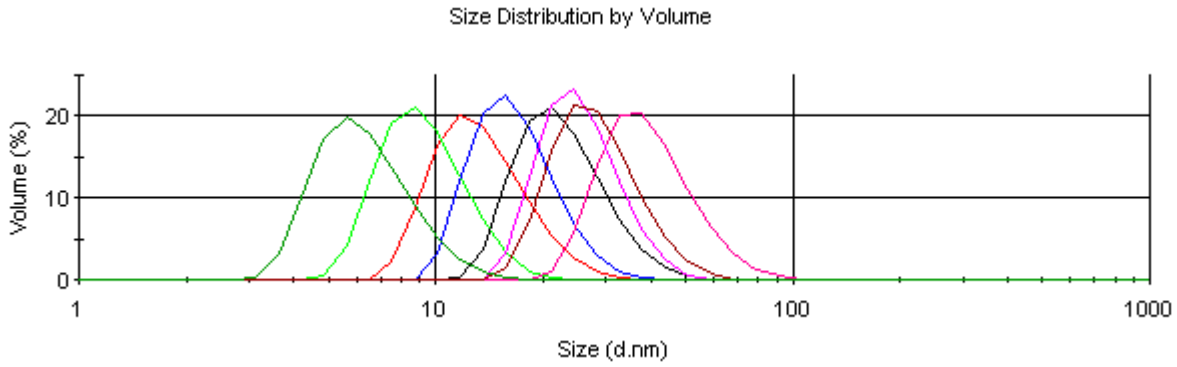

Figure S1. Dynamic Light Scattering measurements for the different core-shell particles in aqueous solution (**[6]** (dark green); **[8]** (light green); **[10]** (red); **[12]** (blue); **[16]** (black); **[18]** (light purple); **[22]** (brown); **[30]** (pink)).

Infrared spectra

(KBr pellets, cm^{-1}): 3650 (w), 3422 (broad), 2956 (sh), 2920 (s), 2874 (sh), 2850 (s), 2172 (m), 2127 (w), 1655 (sh), 1616 (m), 1486 (m), 1468 (s), 1419 (w), 1378 (w), 1440 (w), 992 (w), 721 (w), 667 (w), 492 (s), 450 (sh).

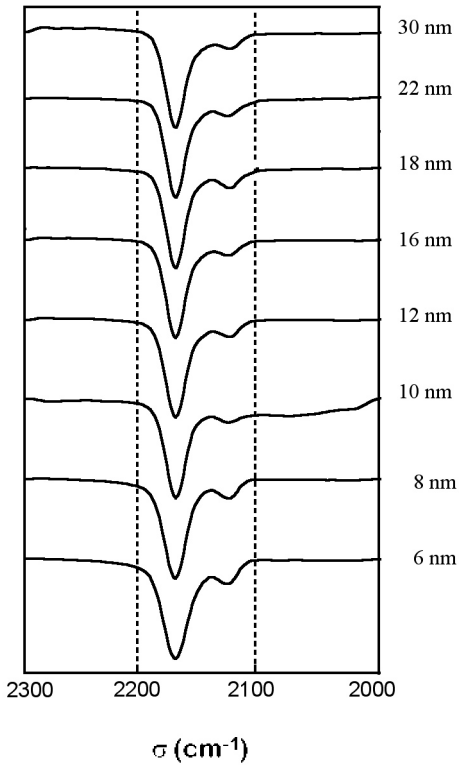

Figure S2. Infra red spectra of the different samples showing the presence of bridging and non-bridging cyanides at 2172 and 2130 cm^{-1} respectively.

X-Ray Powder Diffraction

The XRD powder patterns of the CsNiCr nanoparticles display a face centered cubic structure (*Fm*3*m*) with a lattice constant a = 10.51 Å. The nanoparticles' sizes calculated from the (200) Bragg reflection using Sherrer's formulae are 6.5, 8.3, 11.8, 16.1, 18.2, 21.1 and 27.7 nm for the CsNiCr nanoparticles of theoretical sizes 6, 8, 12, 16, 18, 22 and 30 nm respectively (see Table 1)

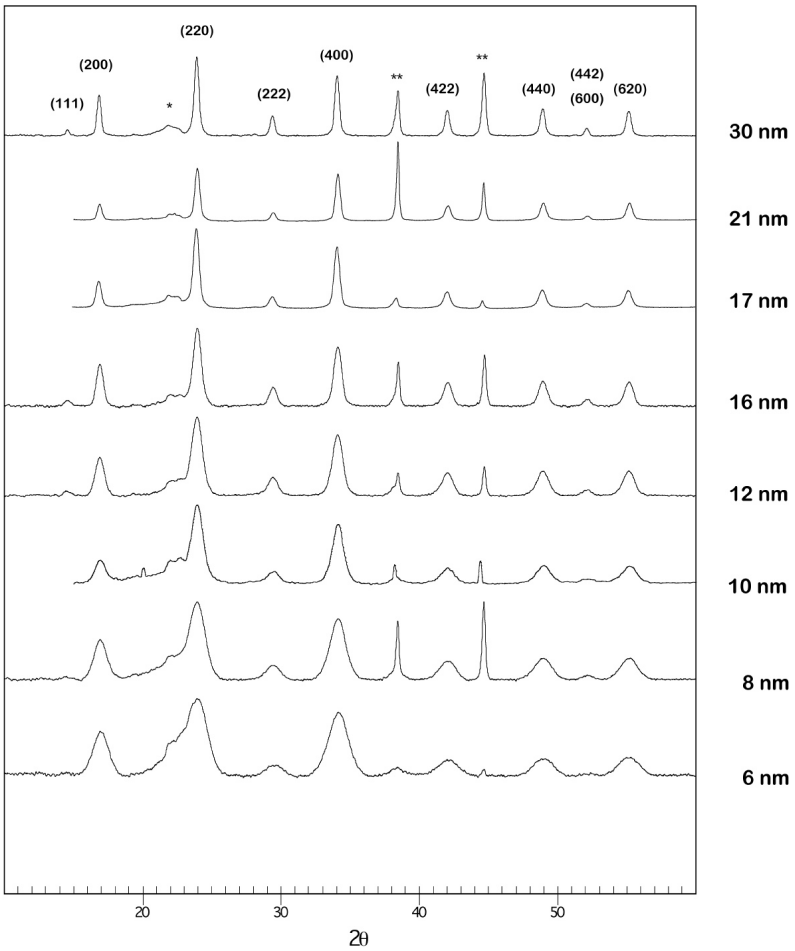

Figure S3. XRPD diagrams of the different samples. * *from DODA and* ** *from the sample holder.*

Elemental analysis on the samples isolated by the addition of DODABr

[6]: $Cs_{0,45}Ni[Cr(CN)_6]_{0,95}(C_{38}H_{80}N)_{0,4}(H_2O)_4$ (M= 607.45 $gmol^{-1}$); calcd (%) for $C_{20.9}H_{40}Cr_{0.95}Cs_{0.45}N_{6.1}NiO_4$: H 6.58, C 41.28, N 14.06, Cr 8.13, Ni 9.55, Cs 9.85; found: H 6.68, C 41.71, N 13.51, Cr 8.33, Ni 9.47, Cs 9.85.

[8]: $Cs_{0,53}Ni[Cr(CN)_6]_{0,97}(C_{38}H_{80}N)_{0,38}(H_2O)_4$ (M= 611.25 $gmol^{-1}$); calcd (%) for $C_{20.26}H_{38.4}Cr_{0.97}Cs_{0.53}N_{6.2}NiO_4$: H 6.28, C 39.77, N 14.20, Cr 8.25, Ni 9.49, Cs 11.53; found: H 6.24, C 39.88, N 13.96, Cr 8.47, Ni 9.60, Cs 11.61.

[10]: $Cs_{0,53}Ni[Cr(CN)_6]_{0.99}(C_{38}H_{80}N)_{0.44}(C_{38}H_{80}NBr)_{2.9}(H_2O)_6$ (M= 2515.46 $gmol^{-1}$); calcd (%) for $C_{132,86}H_{279,2}Br_{2,9}Cr_{0,99}Cs_{0,53}N_{9,28}NiO_6$: H 11.18, C 63.43, N 5.16, Cr 2.04, Ni 2.33, Cs 2.80; found: H 11.1, C 63.2, N 5.27, Cr 2.09, Ni 2.37, Cs 2.85. Residue of DODABr were found for this simple, probable because of insufficient washing. But this has no effect at all on the characterisation of the simple.

[12]: $Cs_{0,57}Ni[Cr(CN)_6]_{0,97}(C_{38}H_{80}N)_{0,34}(H_2O)_{3,5}$ (M=585.57 $gmol^{-1}$); calcd (%) for $C_{18.74}H_{34.2}Cr_{0.97}Cs_{0.57}N_{6.16}NiO_{3.5}$: H 5.84, C 38.40, N 14.73, Cr 8.61, Ni 9.90, Cs 12.94; found: H 5.73, C 38.48, N 14.64, Cr 8.75, Ni 9.92, Cs 12.86.

[16]: $Cs_{0,53}Ni[Cr(CN)_6]_{0,94}(C_{38}H_{80}N)_{0,29}(H_2O)_{2,8}$ (M= 533.91 $gmol^{-1}$); calcd (%) for $C_{16.66}H_{28.8}Cr_{0.94}Cs_{0.53}N_{5.93}NiO_{2.8}$: H 5.39, C 37.44, N 15.55, Cr 9.15, Ni 10.86, Cs 13.20; found: H 5.37, C 37.73, N 14.92, Cr 9.44, Ni 10.82, Cs 13.08.

[18]: $Cs_{0,51}Ni[Cr(CN)_6]_{0,99}(C_{38}H_{80}N)_{0,46}(H_2O)_3$ (M= 640.02 $gmol^{-1}$); calcd (%) for $C_{23,42}H_{42,8}Cr_{0,99}Cs_{0,51}N_{6,4}NiO_3$: H 6.74, C 43.95, N 14.00, Cr 8.04, Ni 9.17, Cs 10.59; found: H 6.65, C 43.3, N 13.9, Cr 7.79, Ni 8.89, Cs 10.73.

[22]: $Cs_{0.5}Ni[Cr(CN)_6]_{0,97}(C_{38}H_{80}N)_{0,41}(H_2O)_3$ (M= 606.97 $gmol^{-1}$); calcd (%) for $C_{21,4}H_{38,8}Cr_{0,97}Cs_{0,5}N_{6,23}NiO_3$: H 6.44, C 42.34, N 14.37, Cr 8.31, Ni 9.67, Cs 10.94; found: H 6.5, C 42.1, N 14.3, Cr 8.01, Ni 9.29, Cs 11.0.

[30]: $Cs_{0,52}Ni[Cr(CN)_6]_{0,97}(C_{38}H_{80}N)_{0,39}(H_2O)_3$ (M= 597.42 $gmol^{-1}$); calcd (%) for $C_{20.64}H_{37.2}Cr_{0.97}Cs_{0.52}N_{6.21}NiO_3$: H 6.23, C 41.46, N 14.55, Cr 8.44, Ni 9.71, Cs 11.57; found: H 6.34, C 41.28, N 14.01, Cr 8.74, Ni 9.71, Cs 11.31.

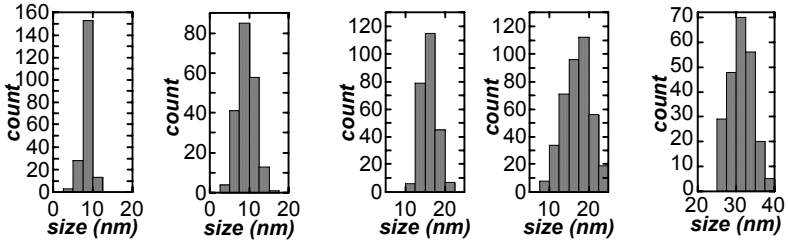

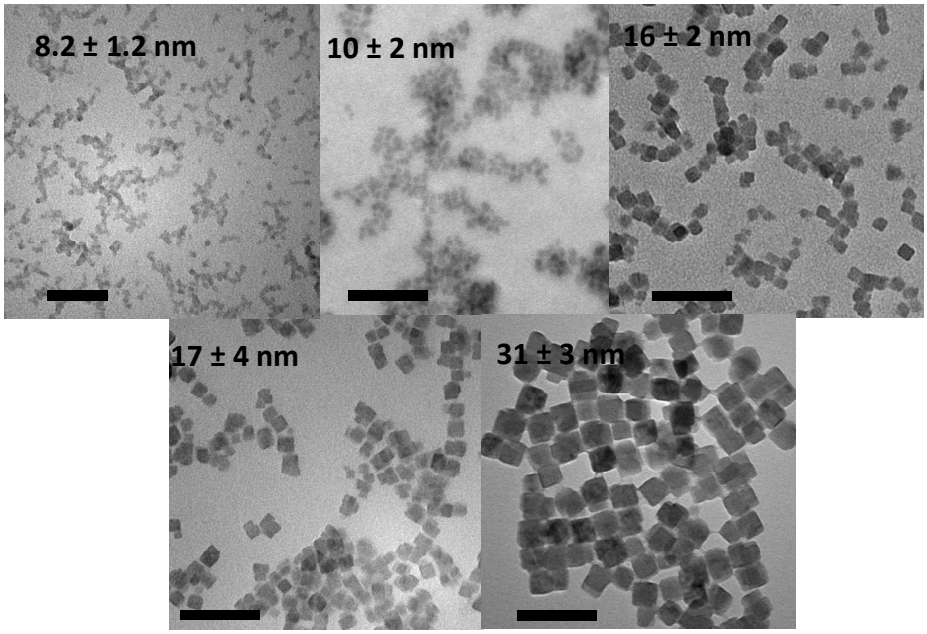

Figure S4. TEM images for samples [8], [10], [16], [18] and [30] (scale bars 100 nm) and size distributions diagrams

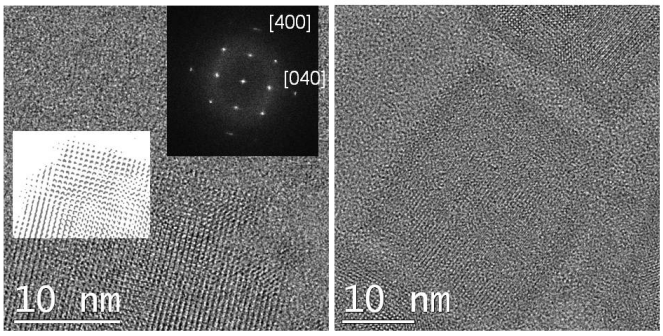

Figure S5. HRTEM images of 30 nm particles and diffraction pattern showing the *fcc* structure.

Magnetisation studies

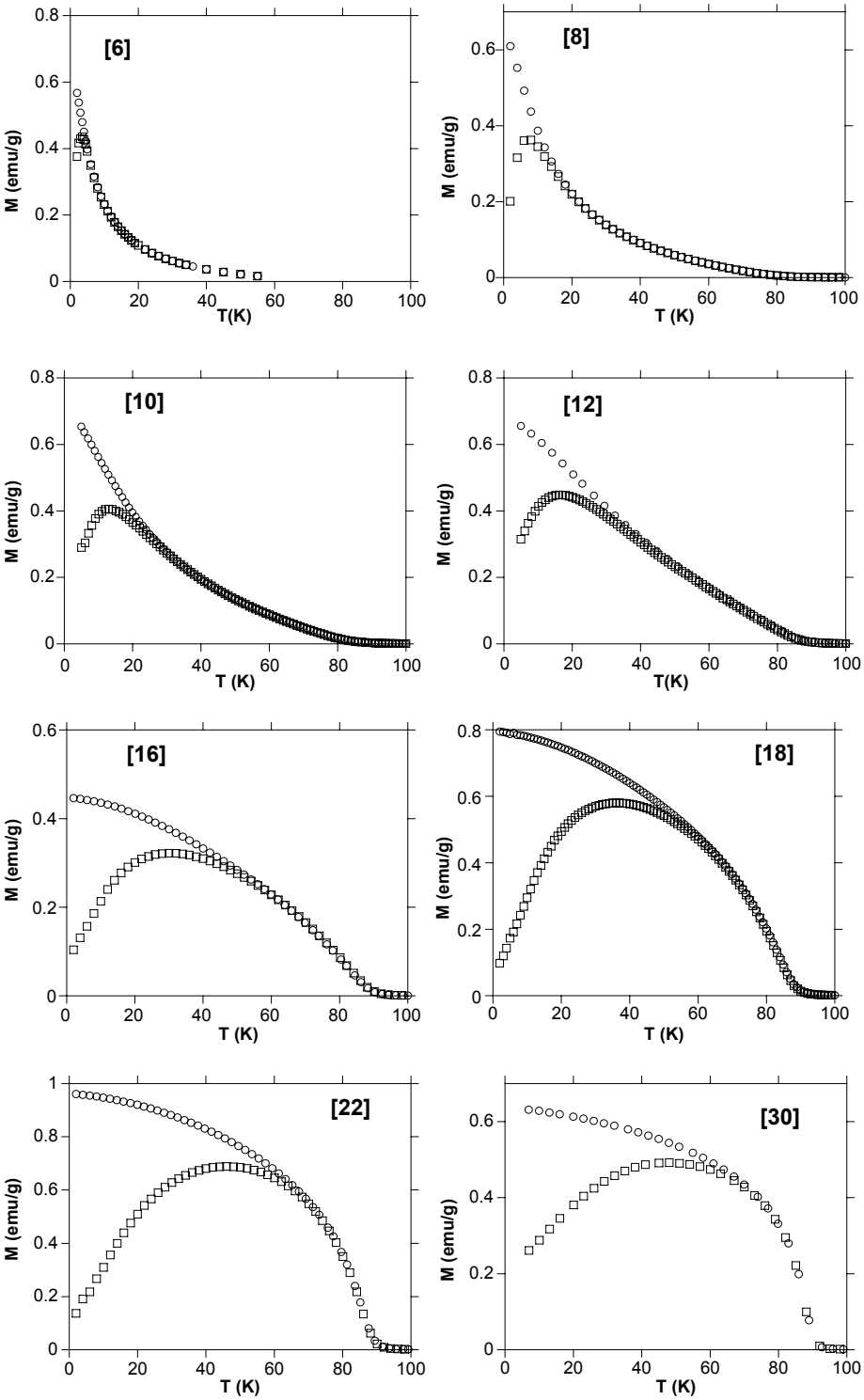

Figure S6. Field cooled (O) and Zero-field cooled (□) magnetization curves for samples **[6], [8]**, **[10]**, **[16]**, **[18], [22]** and **[30]** under an applied field of 30 Oe.

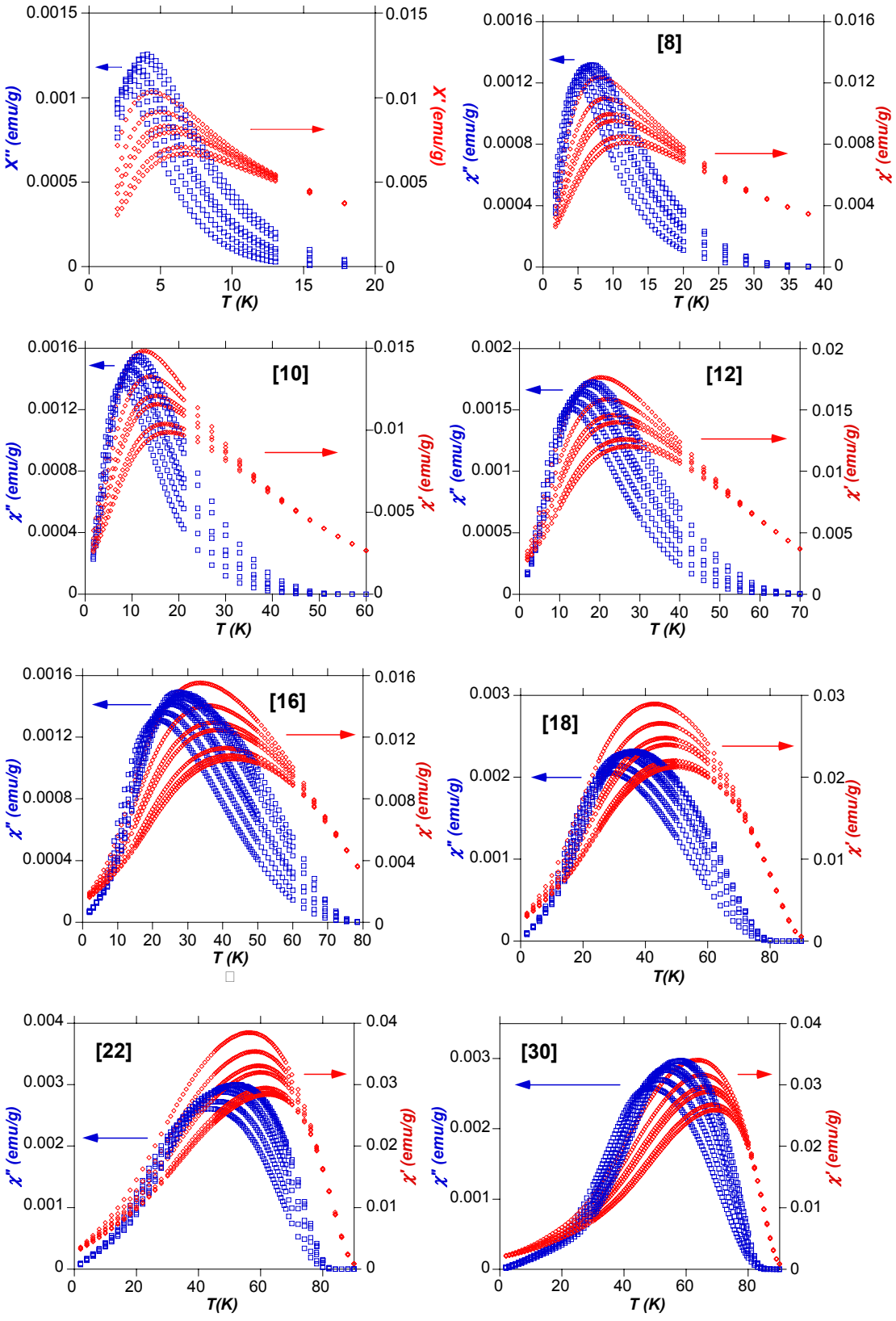

Figure S7. In-phase χ' and out-of-phase χ'' magnetic susceptibilities *vs.* temperature at 1, 10, 50, 100, 500 and 1000 Hz for the different samples.

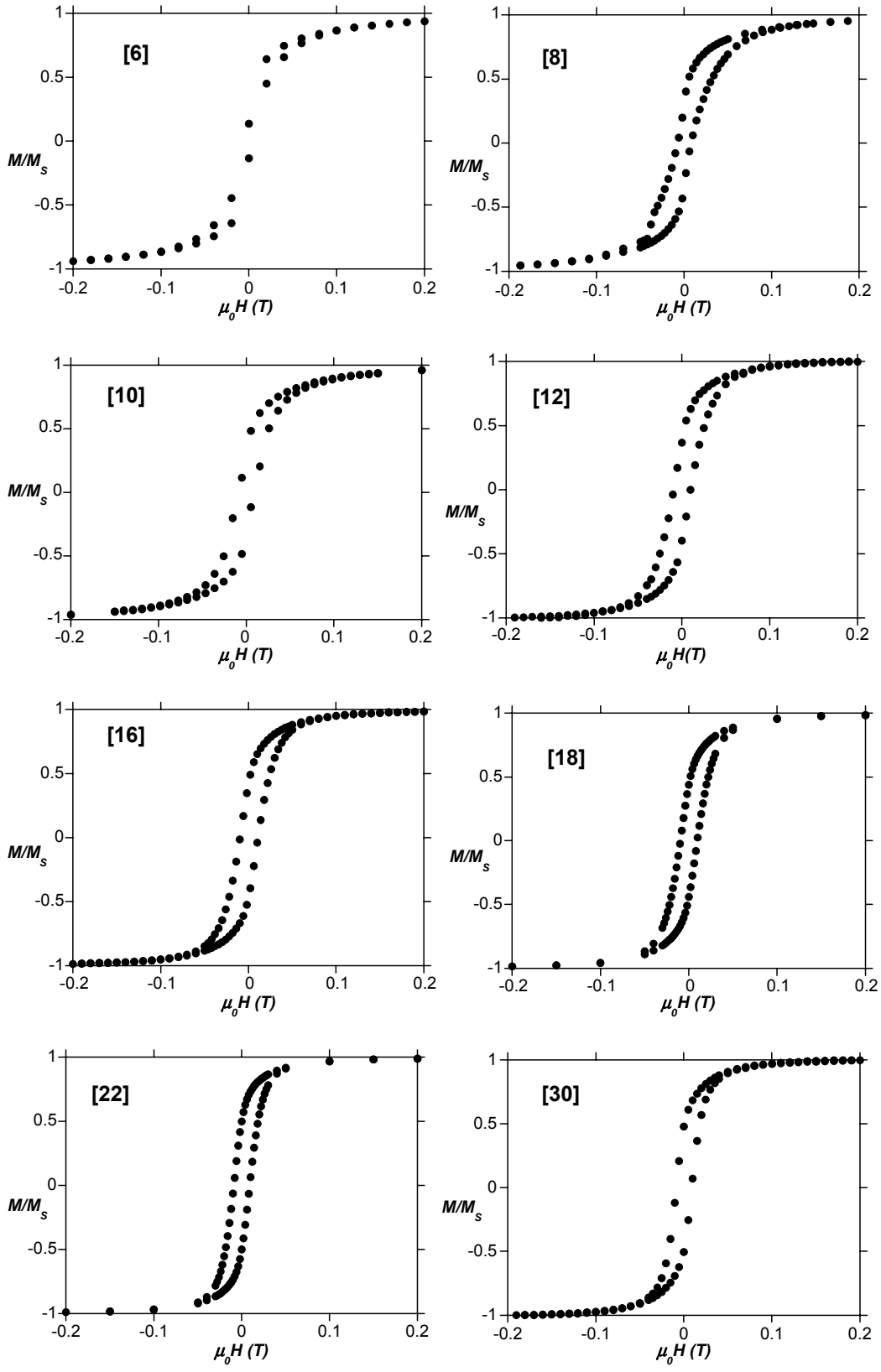

Figure S8. Hysteresis loops for the different samples at T = 2K